Journal of **N**onlinear **A**nalysis and **O**ptimization
Vol. 14, Issue. 2 : 2023
ISSN : **1906-9685**

Genetic Algorithm Optimized CNN for Brain Tumor Segmentation Using Double Density Wavelet Features

Satya Sobhan Panigrahi,Nilachakra Dash,Allupati Chakradhar Patro
Dept. of Computer Science and Engineering, Gandhi Institute For Technology, Bhubaneswar, 752054, India Email: allupati@gift.edu.in

ABSTRACT

Image segmentation is often faced by low contrast, bad boundaries, and inhomogeneity that made it difficult to separate normal and abnormal tissue. Therefore, it takes long periodto read and diagnose brain tumor patients. The aim of this study was to applied hybrid methods to optimize segmentation process of magnetic resonance image of brain. In this study, we divide the brain tumor images with double density dual-tree complex wavelet transform (DDDTCWT), continued by convolutional neural network (CNN), and optimized by genetic algorithm (GA) with 48 combinations yielding excellent results. The F-1 score was 99.42%, with 913 images test data. The training images consist of 1397 normal magnetic resonance imaging (MRI) images and 302 tumor MRI images resized by 32 x32 pixels. The DDDTCWT transforms the input images into more detail than ordinary wavelet transforms, and the CNNs will recognize the pattern of the output images. Additionally, we applied the GA to optimize the weights and biases from the first layer of the CNNs layers. The parameters used for evaluating were dice similarity coefficient (DSC), positive present value (PPV), sensitivity, and accuracy. The result showed that the combination of DDDTCWT, CNN, and GA could be used to brain MRI images and it generated parameters value more that 95%.

1. INTRODUCTION

Magnetic resonance imaging (MRI) is a radiological scanning technique that uses magnets, radio waves, and computers to produce images of body structures [1]. Various methods can be used for imaging a medical object, such as angiogram, brain scan, computerized tomography (CT)-scan, diffusion tensor imaging, functional magnetic resonance imaging (fMRI) [2], MRI, magnetic resonance spectroscopy (MRS), positron emission tomography (PET), and Biopsy [3]. Some literature states that MRI is the best examination tool for its relatively safe radiation hazards [4] and the high accuracy rate. In an MRI examination, the patient is placed on a bed and inserted into a magnetic tube. A strong magnetic field will be formed and align the protons of the hydrogen atoms, which are then exposed to radio waves. The receiver would detect the signal on the MRI machine, then the computer would process the received information and produces an image. The images and resolution of MRI are presented in detail and can detect small changes in the body structures. In some procedures, a contrast material, such as gadolinium, is used to improve image accuracy. In addition, MRI can demonstrate the presence of abnormal tissue with high resolution and good contrast [5]. Furthermore, MRI results have a higher sensitivity for detecting the presence or change in tumor size. A tumor is a disease that arises due to abnormal changes in body tissue cells that turn into tumor cells. When a brain tumor occurs, the excessive growth of unnecessary cells causes an increased volume and damage to other cells and interferes with the function of that part of the brain. Brain tumors can cause complications, including cerebral edema, hydrocephalus, brain herniation, epilepsy, and metastases to other places in several areas of the brain, such as the temporal lobe, frontal lobe, parietal lobe [6]. In the case of brain anatomy, MRI uses strong magnetic fields, radio waves, and computers to produce more distinct and detailed images of the brain and skull structures than other methods.

Segmentation is one of the methods in digital image processing besides image compression, restoration, analysis, and others. The segmentation process of brain tumor MRI images aims to divide the area of the MRI image based on the features (color, texture, density, contrast, and other features) [7]. The accuracy of the segmentation results can be used for medical analysis processes such as tumor detection based on the areas formed. The image segmentation results can also be in the form of an area called a region of interest (RoI). The problems faced by MRI image quality for the brain and other organs affect the segmentation process to find RoI. Some of them include having bad boundaries. These bad boundaries may lead to either

inhomogeneity or different intensity ranges, making it challenging to spot the differences between pixels in the image [8]. The pixel intensity in the tumor area tends to overlap with pixels in adjacent normal tissue.

The complexity of the MRI image as the structure and morphology of the human brain is very complex, brain MRI images tend to have low contrast [9], [10], a relatively large manual segmentation time. It requires very high accuracy so that no pixel is missed considering that each pixel contains important information, and in some cases, different MRI images show distinct complexity even though they represent the same tumor type. In addition, the MRI will produce many images as it is captured from various angles (axial, coronal, and sagittal). This can trigger differences of opinion from different experts and the length of time it takes to read the entire image.

Based on the explanations, this study targets to propose a segmenting method for brain MRI images. Segmentation of brain MRI images can be served as a crucial early stage to help early detection, increase the accuracy and facilitate [11] the process of diagnosing brain tumors. Ultimately, it will help to identify the most appropriate type of brain-related treatment.

The development of the brain MRI image segmentation method begins with low-level techniques, such as thresholding [12] and region growing techniques. The thresholding method would group objects by comparison with one or more other intensity groups. However, this approach cannot accommodate all the pixels of the MRI image. Another method that can be used is the unsupervised learning approach, such as clustering [13] and segmentation [14]. The latest segmentation technique used is the deep learning technique [15]. Deep learning is the development of artificial neural networks in machine learning. Therefore, it can also be called a deep neural network. Deep learning performs the classification of pixels during the segmentation process [16]. The variant of the deep learning technique that has been used is the convolutional neural network (CNN), which accommodates the formation of a learning layer (network) from a set of data automatically. This method classifies each image patch into several classes, such as normal tissue, necrosis, edema, and other classes. This classification aims to label the center point of the voxels [17]. The hybrid method also developed into wavelet method with machine learning [18], and a combination of fully convolutional neural network (FCNN) and conditional random field (CRF) [19].

In line with the development of brain MRI image segmentation methods, it is proposed to combine two or more methods (hybrid method) to segment images. This study proposes a hybrid method by combining the The double density dual-tree complex wavelet transform (DDDTCWT) and CNN with additional genetic algorithm (GA) approaches based on its capabilities and mechanisms.

The combination of these methods will aid each algorithm involved to be more optimal in its implementation DDDTCWT algorithm is a technique that combines double density wavelet transform and dual-tree wavelet transform [20]. The difference between the two only lies in the number of directions (frequency) of the two previous methods so that the results will be more numerous and detailed. The wavelet transform involves n levels of decomposition [21] to extract the features contained in the image using the filtering function. With more features that can be extracted, it will be easier to carry out the following analysis process, including the segmentation process. In this research, DDDTCWT was used to transform the input images in detail. Each level of decomposition with DDDTCWT will involve six filtering functions, which represent low pass filtering and high pass filtering. This detailed decomposition process will identify more feature information contained in the image and increase CNN's recognition and learning process. DDDTCWT can also solve the shift-invariance and directional selectivity. Shift invariant occurs when the

image is shifted, while the directional selectivity means that more information will be extracted as the direction/orientation of the pixel extraction at each level of decomposition.

CNN algorithm can recognize an image through the learning process (courses or training) with a given object. Then, CNN studies all the features in the image through a series of processes, including convolution, activation, pooling, and the formation of a fully connected network (FCN) [22]. There were additional process options during the formation of FCN, namely the optimization of weights and biases involving a GA [23]. Here, we only optimized the first layer of the CNNs with GA and saw its performance. GA works as a natural successive that would produce springs, mutation, cross-product, and so on. In many cases, the FCN algorithm proved can solve an optimization problem [24]. Then, GA will optimize the weights and biases from the first layer of the CNNs layers so that the identification process will be easier and faster. In addition, GA will update the parameter values in the training data process by not doing repetitions. The principle of GA is to select the gene with the best fitness value so that the weight and bias values included in each optimization process (crossovers and mutations) are with optimal values.

2. LITERATURE REVIEW

Several studies have been conducted regarding various proposed algorithms for image segmentation. These algorithms use diverse approaches, such as thresholding, classification, clustering, and hybrid method. Each application of the algorithm gives different accuracy results in the range of 80 - 99%. There are several updates in image segmentation methods, from conventional to hybrid methods. Threshold and region-based approaches are part of the conventional one. Gaussian mixture model algorithm for segmenting brain MRI images is an example of applying a region-based approach [25]. Another study in 2016 that used the threshold concept was the magnitude base multilevel method [12]. Moreover, some studies use the concept of supervised and unsupervised learning for brain MRI image segmentation using the adaptive K-Means Clustering method and the support vector machine (SVM) method [26]. An unsupervised learning method that combines fuzzy c-means with k-means clustering has also been studied in India [27] from 2018 to 2020, several researchers combined one or more techniques to help identify the presence of brain tumors, such as combining a discrete wavelet transform with a probabilistic neural FCN [28] and fully convolutional neural network (FCNNs) with CRF [29]. The following Table 1 shows several previous studies with different methods.

Table 1. Segmentation methods used in previous research

No	Research	Method	DSC (%)	PPV (%)	Sensitivity (%)
1	Havaei [9]	Deep Neural Network	88	89	87
2	Kamnitsas [29]	Fully Connected CRF	89.8	-	89.1
3	Tustison [29]	Concatenad Random Forest	87	85	89
4	Kwon [29]	Combining Generative Model	88	92	84
5	Pereira [30]	Convolutional Neural Network	88	88	89
6	Zhao [30]	FCNNs dan CRF	87	92	83
7	Shen [30]	Fully Convolution Network	87	85	89
8	Senthilkumar [31]	Back Propagation Neural Network	-	-	89

3. METHOD

3.1. Research framework

This section contains an explanation of the research framework, the data used, the proposed image segmentation method, and the performance evaluation technique of the proposed method. This section also describes about input parameter of each algorithm, scenario used for experiment, part of pseudocode for the MATLAB code, and CNN architecture proposed. This study has two problem formulations: (1) how to apply a combination of three methods (DDDTCWT, CNN, and GA) to segment brain MRI images. It means how to combine the workings and input parameters of each method to segment brain MRI images. (2) how is the performance of the proposed method to segment the image and identify the grade of tumor or normal tissue. The performance was evaluated with four indicators: Dice similarity coefficient (DSC), positive present value (PPV), sensitivity, and accuracy as shown in Figure 1. Thus, the purpose of this research is to develop the architecture of the proposed hybrid method into a software and evaluate its performance. This study used several stages to achieve the goal, including literature reviews, conducting simulations/experiments on the developed software, and observing the results of experiments/simulations.

3.2. Samples

The images used in this study were grouped into three, namely training images, testing images, and ground truth images. The training images were used to study the features contained in all the training images

by performing feature extraction. Testing images for examining the image segmentation to produce RoI, and the ground truth images were a collection of testing images that have been segmented by the media or other methods and were utilized as a comparison with the output image segmented by the proposed method. This ground truth image represents the normal image and the tumor image as shown in Figure 2. All MRI images were obtained from several hospitals in Indonesia and the Kaggle website. In total, there were 1699 training images (1397 MRI images of normal patients and 302 for brain tumor patients) and 913 test images (359 tumor MRI images and 554 normal MRI images). 913 images from Kaggle sources were used as ground truth images to compare the output images of the segmentation with the proposed method. The distribution of training images with test images was done randomly by MATLAB with a ratio of 70:30. This study does not specifically use the image sharing approach as the amount of data available was adequate. In addition to training images and testing images,

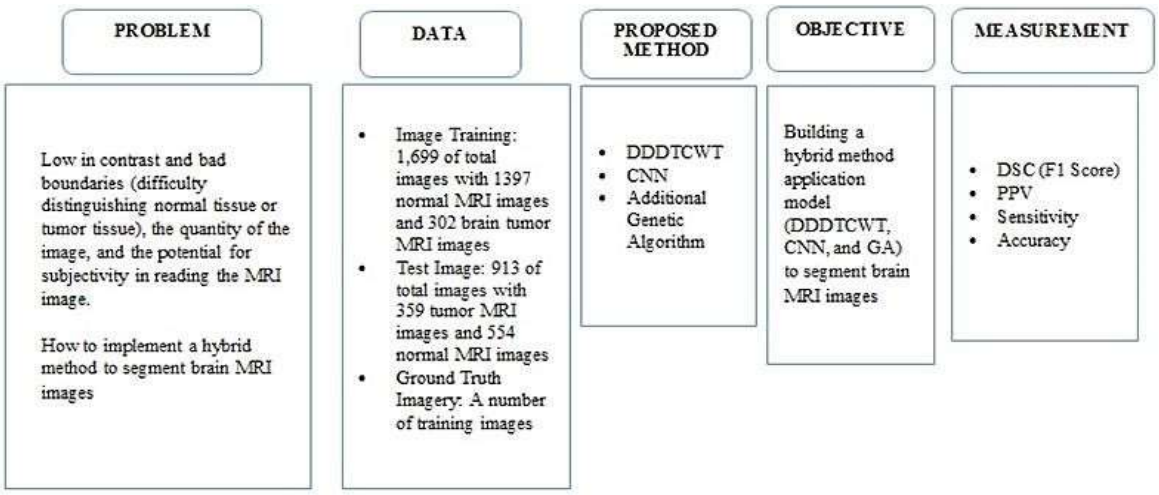

Figure 1. Shows the research framework

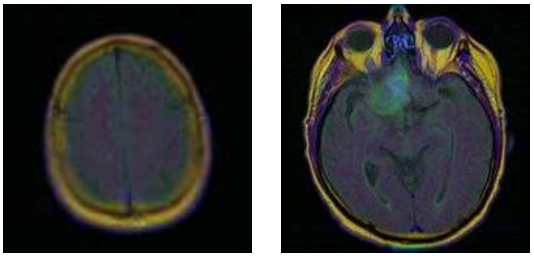

Figure 2. Normal and tumor MRI images (Kaggle)

3.3. Proposed method

The method proposed in this study is a combination of DDDTCWT, CNN, and GA. DDDTCWT is a development of the discrete wavelet transform (DWT) approach with the ability to decompose an image into several sub-images up to the nth level. Every decomposition process will produce four sub-bands, which are approximation sub-band, diagonal detail sub-band, vertical detail sub-band, and diagonal detail sub-band. Image decomposition will be performed on the approximation sub-band because it represents the original image. The decomposition results assist in the extraction of detailed information (features) contained in the image. The more features obtained, the easier the image segmentation process will be. DDDTCWT improves the limitations of DWT in addressing the directional selectivity. DDDTCWT can accommodate a shifting image (invariance translation) and more extraction from image pixels (directional selectivity). The input parameters used by the DDDTCWT method for the segmentation process are the level of decomposition and the wavelet function. In this study, the levels of decomposition used were level 1 to level 5. Meanwhile, the wavelet function used three options, including the DDDTCWT filter function (dddtf1), self1 and self2 filter functions (for the wavelet transform approach).

The same goes for the multi-layer convolution approach in the deep learning method. CNN is trained to understand the details of an image better as it works on the principle of multi-layer. Thus, CNN is able to learn to identify the different features or details of an image distinctively. The CNN algorithm would carry out the learning process of all the features in the training image obtained from the extraction by DDDTCWT. After CNN learns the features contained in the training image, 60 FCN scenarios will be formed. The input parameters for the CNN algorithm were the convolution layer, activation function, pooling, and optimization function. The parameter values of the proposed activation function were rectified linear units (RELU) and hyperbolic tangent (TANH) functions, as both are easy to perform and do not cause large computations, with the consideration that the data used was adequate. This activation function was expected to obtain a convergent state quickly. Table 2 shows a list of the input parameters used from the algorithms involved.

Table 2. Input parameters of each algorithm to form FCN

No	Input Parameter	Instance	Information
1	Decomposition Level	1-5	Decomposition level up to 5 according to the size of the training image. In addition, a greater level of decomposition will take more time.
2	Wavelet Function	DDDTF1 SELF1 SELF2	Double Density Dual Tree Filtering 1 (DDDTF1) is the filter function of the DDDTCWT method, while SELF1 and SELF2 are wavelet functions of other wavelet transforms.
3	Number of Convolutions	According to requirements	In each experiment, the number of convolutions can be determined as desired. Referring to previous research, the number of convolutions can be done more than once.
4	Convolution Matrix Size	2x2 or 3x3	The proposed matrix size from previous research
5	Activation Function	Relu Function Tanh Function	RELU function is the most common used to perform activation.
6	Pooling Technique	Max Pooling Average Pooling	The second pooling technique is proposed from previous research through literature study.
7	Optimization (GA)	Yes (With GA) No (NO GA)	Yes: To build a neural network, it is necessary to optimize the weight of each layer. No: To build a neural network, there is no need to optimize the weight of each layer.

Next, the parameter values for the optimization function (optimization of weights and biases) were applied with or without GA, and MAX pooling was used as the default of the CNN algorithm. Max pooling is a pooling parameter value that has been widely used in medical image analysis and provides an average accuracy of 90-98%. Table 3 shows four FCN scenarios from the training results, which resulting 60 schemes.

Before the formation of a neural network, the weight value of each input layer and hidden layer is required. During the convolution process, the weight and bias value optimization was performed by applying the GA algorithm. GA aids to gain optimal weight and bias values from all iterations (epochs) that occurred. Figure 3 is a CNN architecture chart for the training process from the previous method with DDDTCWT. Generally, DDDTCWT performs decomposition, filtering, and re-decomposition (reformat of the image). The following is the pseudocode for DDDTCWT used in this study.

```
Step 1: Decomposition
#Determining the Decomposition Level #Level 1...4
Step 2: Filtering
#Wavelet function call case 1
level=1; dtcplx=dddtree2(typetree,grayImage,level,filtername); dtcplx.cfs{2} =
zeros(size(dtcplx.cfs{2}));
end Case
4
level = 4;
dtcplx = dddtree2(typetree,grayImage,level,filtername); dtcplx.cfs{1} =
zeros(size(dtcplx.cfs{1})); dtcplx.cfs{2} = zeros(size(dtcplx.cfs{2}));
dtcplx.cfs{3} = zeros(size(dtcplx.cfs{3})); dtcplx.cfs{5} =
zeros(size(dtcplx.cfs{5}));
end
Step 3: Re-decomposition Image #dtImage =
idddtree2(dtcplx);
```

Table 3. FCN formation scenario

No	SCENARIO		
		RELU NO GA	
	DDDDTF1	SELF1	SELF2
Scenario 1	Decomposition Level 1	Decomposition Level 1	Decomposition Level 1
	Decomposition Level 2	Decomposition Level 2	Decomposition Level 2
	Decomposition Level 3	Decomposition Level 3	Decomposition Level 3
	Decomposition Level 4	Decomposition Level 4	Decomposition Level 4
	Decomposition Level 5	Decomposition Level 5	Decomposition Level 5
		TAHN NO GA	
	DDDDTF1	SELF1	SELF2
Scenario 2	Decomposition Level 1	Decomposition Level 1	Decomposition Level 1
	Decomposition Level 2	Decomposition Level 2	Decomposition Level 2
	Decomposition Level 3	Decomposition Level 3	Decomposition Level 3
	Decomposition Level 4	Decomposition Level 4	Decomposition Level 4
	Decomposition Level 5	Decomposition Level 5	Decomposition Level 5
		RELU WITH GA	
	DDDDTF1	SELF1	SELF2
Scenario 3	Decomposition Level 1	Decomposition Level 1	Decomposition Level 1
	Decomposition Level 2	Decomposition Level 2	Decomposition Level 2
	Decomposition Level 3	Decomposition Level 3	Decomposition Level 3
	Decomposition Level 4	Decomposition Level 4	Decomposition Level 4
	Decomposition Level 5	Decomposition Level 5	Decomposition Level 5
Scenario 4		TAHN WITH GA	
	DDDDTF1	SELF1	SELF2
	Decomposition Level 1	Decomposition Level 1	Decomposition Level 1
	Decomposition Level 2	Decomposition Level 2	Decomposition Level 2
	Decomposition Level 3	Decomposition Level 3	Decomposition Level 3
	Decomposition Level 4	Decomposition Level 4	Decomposition Level 4
	Decomposition Level 5	Decomposition Level 5	Decomposition Level 5

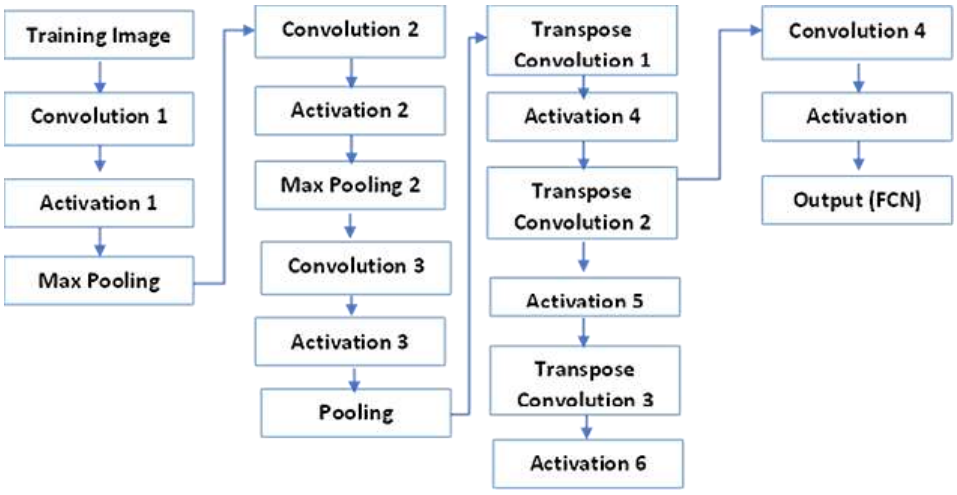

Figure 3. CNN layer architecture

3.4. Evaluation method

The performance of the proposed hybrid method was evaluated with four indicators, namely DSC [32] or F-1 score, PPV, sensitivity, and accuracy. The first three values measure the results of the comparison between the segmented image by the proposed method and the ground truth image, while the last indicator for the ability of the algorithm to detect the class (tumor/normal) of the segmented image. These four values were obtained through the values of true positive (TP), false positive (FP), true negative (TN), and false negative (FN) in the confusion matrix [33]. The formula to measure the four indicator values are,

$$DSC = \frac{2xTP}{(TP+FN)+(TP+FP)} \quad (1)$$

$$PPV = \frac{TP}{(TP+FP)} \quad (2)$$

$$Sensitivity = \frac{TP}{(TP+FN)} \quad (3)$$

$$Accuracy = \frac{TP+TN}{(TP+FP+FN+TN)} \quad (4)$$

Where:

DSC	= Dice Similarity Coefficient
PPV	= Present Positive Value
Sensitivity	= Sensitivity
Accuracy	= Accuracy
TP	= True Positive
TN	= True Negative
FP	= False Positive
FN	= False Negative

4. RESULTS AND DISCUSSION

The output of this research is a software of the proposed hybrid method architecture and its performance evaluation. MATLAB apps were used to segment brain MRI images as shown in Figure 3 with the proposed hybrid method as it provides the toolbox needed and is easy to use, such as wavelet transform, machine learning, and deep learning. Furthermore, MATLAB works on a matrix-based, making it easier to learn how the compiled program works. Previous studies had published output in an architectural design for the combined application of these three methods [34]. The hybrid method architecture was developed through three major processes, namely training, testing, and evaluation. The training process aims to conduct learning on all training images based on the contained features. Concluding on how each method works, the input parameters involved, and the value of each input parameter, this study proposes four scenarios that produce 60 FCN combinations. The input parameters for the DDDTCWT algorithm are the level of decomposition and the filtering function used. The proposed decomposition levels ranged from 1 to 5 with three filtering functions, namely the filter function DDDTF1, SELF1, and SELF2. DDDTF1 is a wavelet filter function recommended for DDDTCWT, while SELF1 and SELF2 are the default filter functions of the wavelet transform and are available in the MATLAB library. FCN is a representation of the learning outcomes of the proposed method on the features contained in all training images.

These 60 FCN combinations were then tested on 913 images, yielding the performance value of the proposed hybrid method. Tables 4 to 7 respectively show the performance of the methods according to the combination in Table 1. Aided by the formed FCN, each test image will be segmented one by one while still entering the input parameters according to the FCN used. In other words, this process goals to test the learning outcomes (FCN) in recognizing the features and can segment or form RoI from each of the testing images. Figure 4 is the graphical user interface (GUI) of the proposed method in MATLAB. Based on Figure 4, the left side is the part for entering the input parameter values from the DDDTCWT algorithm and calling the FCN that has been generated from the training process. It also presents the performance of the proposed method in four indicators, namely DSC, PPV, sensitivity, and accuracy. The right side respectively represents the test image used, the segmented image using the DDDTCWT algorithm, RoI from the test image of the hybrid method, RoI from the ground truth image, and the segmented image by the hybrid method.

Table 4. Performance of scenario 1

No.	1	2	3	4	5	6	7	8	9	10	11	12	13	14	15
								RELU Not GA							
Measurement		dddtf1					self1						self2		
	LD1	LD2	LD3	LD4	LD5	LD1	LD2	LD3	LD4	LD5	LD1	LD2	LD3	LD4	LD5
DSC (%)	98.19	98.53	98.61	98.77	98.75	97.87	98.29	98.52	98.70	98.54	98.29	98.57	98.63	98.32	98.43
PPV (%)	97.51	98.02	98.02	98.37	98.22	96.82	97.66	97.94	98.39	97.93	97.70	98.18	98.22	97.71	97.55
Sensitivity (%)	98.96	99.11	99.28	99.24	99.32	99.02	99.01	99.16	99.07	99.22	98.95	99.02	99.10	99.07	99.39
Accuracy (%)	96.54	97.17	97.34	97.65	97.60	95.93	96.72	97.17	97.51	97.19	96.71	97.24	97.37	96.79	97.00

Table 5. Performance of scenario 2

No.	16	17	18	19	20	21	22	23	24	25	26	27	28	29	30
	TANH Not GA														
Measurement	dddtf1					self1					self2				
	LD1	LD2	LD3	LD4	LD5	LD1	LD2	LD3	LD4	LD5	LD1	LD2	LD3	LD4	LD5
DSC (%)	97.18	98.21	98.04	97.99	98.43	98.29	97.83	98.17	98.43	98.08	98.15	98.03	98.07	97.82	97.81
PPV (%)	95.49	97.28	96.85	96.83	97.56	97.67	96.61	97.17	97.87	96.90	97.37	97.01	97.01	96.62	96.46
Sensitivity (%)	99.09	99.24	99.37	99.29	99.39	98.99	99.20	99.26	99.08	99.36	99.03	99.18	99.23	99.16	99.32
Accuracy (%)	94.69	96.58	96.28	96.17	97.00	96.71	95.87	96.49	97.01	96.34	96.48	96.25	96.32	95.87	95.85

Table 6. Performance of scenario 3

No.	31	32	33	34	35	36	37	38	39	40	41	42	43	44	45
	RELU WITH GA														
Measurement	dddtf1					self1					self2				
	LD1	LD2	LD3	LD4	LD5	LD1	LD2	LD3	LD4	LD5	LD1	LD2	LD3	LD4	LD5
DSC (%)	98.35	98.84	98.45	98.63	98.57	98.28	98.28	98.64	99.42	98.02	98.46	98.56	98.71	98.39	98.69
PPV (%)	97.86	98.62	97.66	98.20	97.95	97.69	97.56	98.27	100.00	97.05	98.03	98.19	98.39	97.83	98.39
Sensitivity (%)	98.94	99.11	99.32	99.13	99.25	98.96	99.08	99.08	98.86	99.09	98.95	99.00	99.07	99.02	99.06
Accuracy (%)	96.85	97.77	97.03	97.37	97.25	96.70	96.70	97.38	98.86	96.19	97.04	97.23	97.51	96.91	97.49

Table 7. Performance of scenario 4

No.	46	47	48	49	50	51	52	53	54	55	56	57	58	59	60
	TANH WITH GA														
Measurement	dddtf1					self1					self2				
	LD1	LD2	LD3	LD4	LD5	LD1	LD2	LD3	LD4	LD5	LD1	LD2	LD3	LD4	LD5
DSC (%)	97.55	98.44	98.41	99.42	98.61	97.57	99.42	98.12	98.32	98.12	96.57	98.22	98.63	98.02	95.93
PPV (%)	96.25	97.73	97.57	100.00	97.95	96.24	100.00	97.09	97.53	97.32	94.17	97.41	98.14	96.98	93.04
Sensitivity (%)	99.01	99.25	99.34	98.86	99.34	99.01	98.86	99.30	99.18	99.02	99.23	99.12	99.16	99.18	99.16
Accuracy (%)	95.35	97.01	96.97	98.86	97.34	95.38	98.86	96.45	96.78	96.40	93.53	96.59	97.37	96.23	92.32

The next output is from measuring the performance of the proposed method for segmenting and detecting the testing images of tumor or normal. The measurement indicators used were DSC, PPV, sensitivity, and accuracy. Based on the first experimental scenario with the FCN formation scheme of RELU activation function without involving GA, the highest DSC and accuracy values were in DDDTF1 wavelet function and decomposition level 4 with 98.7% and 97.65%, respectively. However, the highest sensitivity value (98.39%) was in SELF1 with decomposition level 5. The utmost PPV value was obtained when using the SELF1 filter function with decomposition level 4 with 98.39% as shown in Table 4. Then, the performance of the second scenario, the TANH activation function without GA, shows the highest DSC, PPV, and accuracy values with the fourth decomposition level and wavelet function SELF1, while the highest sensitivity value was in the DDDTF1 of the fifth decomposition level as shown in Table 5. Next, the third scenario involves the RELU activation and the GA optimization function in the FCN formation. Table 6 shows that SELF1 with the fourth decomposition level had the highest DSC, PPV, and accuracy values, while the DDDTF1 with the third decomposition level had the highest sensitivity value. The last scenario involves TANH activation function and the GA optimization had two schemes with the highest DSC, PPV, and accuracy values, namely DDDTF1 with decomposition level 4 and SELF1 with decomposition level 2. Sedangkan nilai akurasi tertinggi ketika menggunakan fungsi filter DDDTF1 dan level dekomposisi 3 as shown in Table 7.

Overall, only scenarios 3 and 4 have PPV values reaching 100%. It proves that the integration of the GA optimization function affects the PPV value, and the scheme without GA shows that the largest PPV value is always at the fourth decomposition level. The highest DSC value also occurs in those scenarios when applying both RELU and TAHN activation functions with GA optimization. Likewise, the highest sensitivity value falls in the scheme of THAN activation function with and without GA. In detail, the highest sensitivity

value lies in the DDDTF1 with the third decomposition level. Lastly, the best accuracy values of 98.86% lie in scenarios three and four, precisely in the SELF1with decomposition level 2 (scenario 3), DDDTF1 with decomposition level 4 (scenario 3), and DDDDTF1 filter function with decomposition level 4 (scenario 4).

Based on its performance, all measurement indicators of the proposed method had scores ranging from 95% to 100%. This shows that the proposed hybrid method provides a better contribution than previous studies to perform image segmentation. This also proves the ability of each method used, CDDDTWT as a variant of the wavelet transform approach, to extract all the features contained in all training images. Moreover, CNN can learn distinctively all features in the images and can produce optimal weight and bias values when integrated with GA.

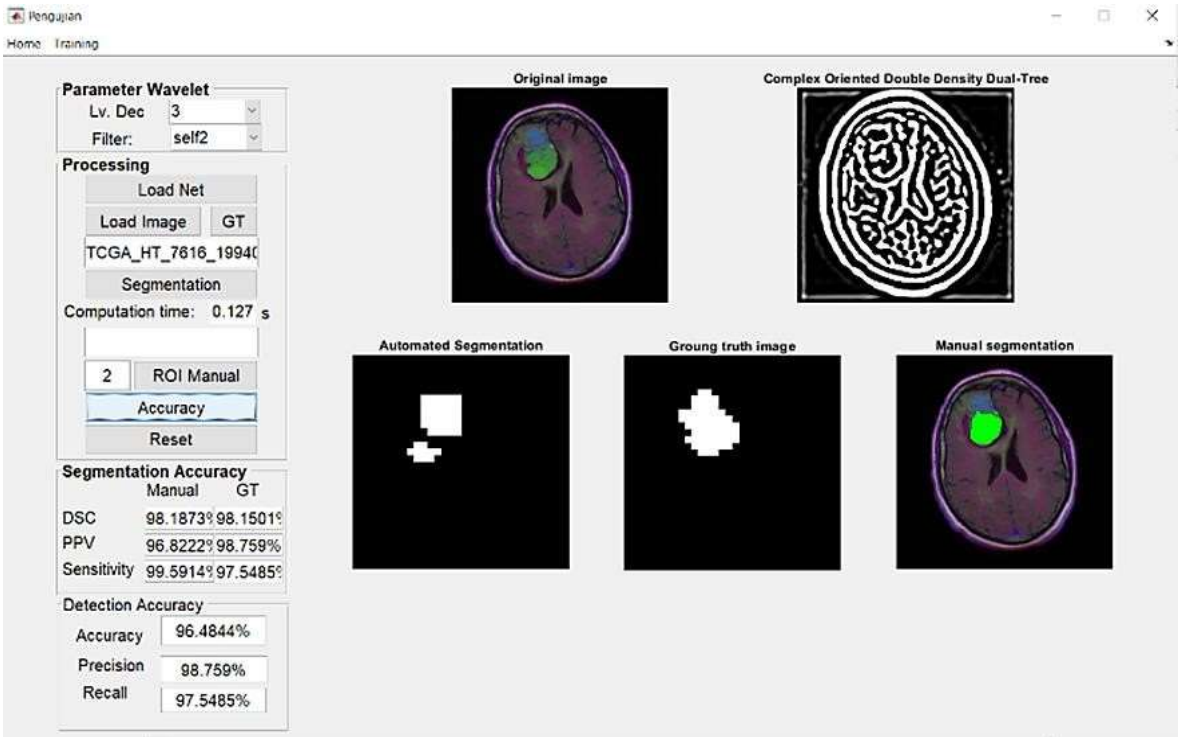

Figure 4. Application of the proposed testing method with the MATLAB tool

5. CONCLUSION

The combination of DDDTCWT, CNN, and GA can be applied to segment brain MRI images. The combination of the mechanisms and capabilities of the three methods shows the success of segmenting brain MRI images with excellent assessment indicators. All combinations of the proposed hybrid system in this study showed more than 95% in all parameters measured (DSC, PPV, sensitivity, and accuracy) using 913 test images. The top 3 combinations were (1) RELU with GA, filter type of DDDTCWT in SELF1 with decomposition level 4, (2) TANH with GA, filter type of DDDTCWT in DDDTF1 with decomposition level 4, and (3) TANH with GA, filter type of DDDTCWT in SELF1 with level decomposition 2. The smallest value found at TANH with GA, filter type of DDDTCWT in SELF2 with level decomposition 1. Adding the GA in the system improved the system measurements on average, although the time consumed by the system to apply GA is doubled. Further improvements of this hybrid method with another technic and CNN training are required for a more applicable technique. In addition, this study also suggests increasing the number of data sets, both training and testing data. Furthermore, if the number of data sets obtained is quite large, it needs the cross-validation technique in the distribution of the image, given that cross-validation can increase the model's performance.

ACKNOWLEDGEMENTS

The authors would like to thank the Kalbis Institute of Technology and Business for funding this research. We would also like to thank Bina Nusantara University for providing the promoter and co-promoter for this research.

REFERENCES

[1] L. Rundo, C. Militello, G. Russo, S. Vitabile, M. C. Gilardi, and G. Mauri, "GTVcut for neuro-radiosurgery treatment planning: an MRI brain cancer seeded image segmentation method based on a cellular automata model," *Natural Computing*, vol. 17, no. 3, pp. 521–536, 2018, doi: 10.1007/s11047-017-9636-z.

[2] H. J. Lee *et al.*, "Concurrent electrophysiological and hemodynamic measurements of evoked neural oscillations in human visual cortex using sparsely interleaved fast fMRI and EEG," *NeuRoImage*, vol. 217, 2020, doi: 10.1016/j.neuRoImage.2020.116910.

[3] A. Wadhwa, A. Bhardwaj, and V. Singh Verma, "A review on brain tumor segmentation of MRI images," *Magnetic Resonance Imaging*, vol. 61, pp. 247–259, 2019, doi: 10.1016/j.mri.2019.05.043.

[4] T. Rajesh, R. S. M. Malar, and M. R. Geetha, "Brain tumor detection using optimisation classification based on rough set theory," *Cluster Computing*, vol. 22, pp. 13853–13859, 2019, doi: 10.1007/s10586-018-2111-5.

[5] S. Koike *et al.*, "Brain/MINDS beyond human brain MRI project: A protocol for multi-level harmonization across brain disorders throughout the lifespan," *NeuRoImage: Clinical*, vol. 30, 2021, doi: 10.1016/j.nicl.2021.102600.

[6] M. L. Tsai *et al.*, "Seizure characteristics are related to tumor pathology in children with brain tumors," *Epilepsy Research*, vol. 147, pp. 15–21, 2018, doi: 10.1016/j.eplepsyres.2018.08.007.

[7] H. Shen, J. Zhang, and W. Zheng, "Efficient symmetry-driven fully convolutional network for multimodal brain tumor segmentation," *Proceedings - International Conference on Image Processing, ICIP*, vol. 2017-September, pp. 3864–3868, 2018, doi: 10.1109/ICIP.2017.8297006.

[8] C. Ma, G. Luo, and K. Wang, "Concatenated and Connected Random Forests with Multiscale Patch Driven Active Contour Model for Automated Brain Tumor Segmentation of MR Images," *IEEE Transactions on Medical Imaging*, vol. 37, no. 8, pp. 1943–1954, 2018, doi: 10.1109/TMI.2018.2805821.

[9] M. Havaei *et al.*, "Brain tumor segmentation with Deep Neural Networks," *Medical Image Analysis*, vol. 35, pp. 18–31, 2017, doi: 10.1016/j.media.2016.05.004.

[10] M. K. Akter, S. M. Khan, S. Azad, and S. A. Fattah, "Automated brain tumor segmentation from mri data based on exploration of histogram characteristics of the cancerous hemisphere," *5th IEEE Region 10 Humanitarian Technology Conference 2017, R10-HTC 2017*, vol. 2018-January, pp. 815–818, 2018, doi: 10.1109/R10-HTC.2017.8289080.

[11] D. Cheng and M. Liu, "Triple crossing," vol. 10541, no. November, pp. 106–113, 2017, doi: 10.1007/978-3-319-67389-9.

[12] T. Kaur, B. S. Saini, and S. Gupta, "A joint intensity and edge magnitude-based multilevel thresholding algorithm for the automatic segmentation of pathological MR brain images," *Neural Computing and Applications*, vol. 30, no. 4, pp. 1317–1340, 2018, doi: 10.1007/s00521-016-2751-4.

[13] A. Min and Z. M. Kyu, "MRI images enhancement and tumor segmentation for brain," *Parallel and Distributed Computing, Applications and Technologies, PDCAT Proceedings*, vol. 2017-December, pp. 270–275, 2018, doi: 10.1109/PDCAT.2017.00051.

[14] G. Karayegen and M. F. Aksahin, "Brain tumor prediction on MR images with semantic segmentation by using deep learning network and 3D imaging of tumor region," *Biomedical Signal Processing and Control*, vol. 66, 2021, doi: 10.1016/j.bspc.2021.102458.

[15] G. Madhupriya, M. Guru Narayanan, S. Praveen, and B. Nivetha, "Brain tumor segmentation with deep learning technique," *Proceedings of the International Conference on Trends in Electronics and Informatics, ICOEI 2019*, vol. 2019-April, pp. 758–763, 2019, doi: 10.1109/icoei.2019.8862575.

[16] R. Chauhan, K. K. Ghanshala, and R. C. Joshi, "Convolutional Neural Network (CNN) for Image Detection and Recognition," *ICSCCC 2018 - 1st International Conference on Secure Cyber Computing and Communications*, pp. 278–282, 2018, doi: 10.1109/ICSCCC.2018.8703316.

[17] P. Ribalta Lorenzo *et al.*, "Segmenting brain tumors from FLAIR MRI using fully convolutional neural networks," *Computer Methods and Programs in Biomedicine*, vol. 176, pp. 135–148, 2019, doi: 10.1016/j.cmpb.2019.05.006.

[18] K. Usman and K. Rajpoot, "Brain tumor classification from multi-modality MRI using wavelets and machine learning," *Pattern Analysis and Applications*, vol. 20, no. 3, pp. 871–881, 2017, doi: 10.1007/s10044-017-0597-8.

[19] X. Zhao, Y. Wu, G. Song, Z. Li, Y. Zhang, and Y. Fan, "A deep learning model integrating FCNNs and CRFs for brain tumor segmentation," *Medical Image Analysis*, vol. 43, pp. 98–111, 2018, doi: 10.1016/j.media.2017.10.002.

[20] O. Prakash, C. M. Park, A. Khare, M. Jeon, and J. Gwak, "Multiscale fusion of multimodal medical images using lifting scheme based biorthogonal wavelet transform," *Optik*, vol. 182, pp. 995–1014, 2019, doi: 10.1016/j.ijleo.2018.12.028.

[21] P. Samundiswary and H. Rekha, "An efficient pass parallel SPIHT based image compression using double density dual tree complex wavelet transform for WSN," *International Journal of Innovative Technology and Exploring Engineering*, vol. 8, no. 12, pp. 2762–2768, 2019, doi: 10.35940/ijitee.L2564.1081219.

[22] S. Albawi, T. A. Mohammed, and S. Al-Zawi, "Understanding of a convolutional neural network," *Proceedings of 2017 International Conference on Engineering and Technology, ICET 2017*, vol. 2018-January, pp. 1–6, 2018, doi: 10.1109/ICEngTechnol.2017.8308186.

[23] U. K. Acharya and S. Kumar, "Genetic algorithm based adaptive histogram equalization (GAAHE) technique for medical image enhancement," *Optik*, vol. 230, 2021, doi: 10.1016/j.ijleo.2021.166273.

[24] Ö. İnik, M. Altiok, E. Ülker, and B. Koçer, "MODE-CNN: A fast converging multi-objective optimization algorithm for CNN-based models," *Applied Soft Computing*, vol. 109, 2021, doi: 10.1016/j.asoc.2021.107582.

[25] J. Qiao *et al.*, "Data on MRI brain lesion segmentation using K-means and Gaussian Mixture Model-Expectation Maximization," *Data in Brief*, vol. 27, 2019, doi: 10.1016/j.dib.2019.104628.

[26] D. R. Nayak, R. Dash, and B. Majhi, "Pathological brain detection using curvelet features and least squares SVM," *Multimedia Tools and Applications*, vol. 77, no. 3, pp. 3833–3856, 2018, doi: 10.1007/s11042-016-4171-y.

[27] B. Al Kindhi, T. A. Sardjono, M. H. Purnomo, and G. J. Verkerke, "Hybrid K-means, fuzzy C-means, and hierarchical clustering for DNA hepatitis C virus trend mutation analysis," *Expert Systems with Applications*, vol. 121, pp. 373–381, 2019, doi: 10.1016/j.eswa.2018.12.019.

[28] N. Varuna Shree and T. N. R. Kumar, "Identification and classification of brain tumor MRI images with feature extraction using DWT and probabilistic neural network," *Brain Informatics*, vol. 5, no. 1, pp. 23–30, 2018, doi: 10.1007/s40708-017-0075-5.

[29] K. Kamnitsas *et al.*, "Efficient multi-scale 3D CNN with fully connected CRF for accurate brain lesion segmentation," *Medical Image Analysis*, vol. 36, pp. 61–78, 2017, doi: 10.1016/j.media.2016.10.004.

[30] S. Pereira, A. Pinto, V. Alves, and C. A. Silva, "Brain Tumor Segmentation Using Convolutional Neural Networks in MRI Images," *IEEE Transactions on Medical Imaging*, vol. 35, no. 5, pp. 1240–1251, 2016, doi: 10.1109/TMI.2016.2538465.

[31] C. Senthilkumar and R. K. Gnanamurthy, "A Fuzzy clustering based MRI brain image segmentation using back propagation

neural networks," *Cluster Computing*, vol. 22, pp. 12305–12312, 2019, doi: 10.1007/s10586-017-1613-x.

[32] C. E. Cardenas *et al*., "Deep Learning Algorithm for Auto-Delineation of High-Risk Oropharyngeal Clinical Target Volumes With Built-In Dice Similarity Coefficient Parameter Optimization Function," *International Journal of Radiation Oncology Biology Physics*, vol. 101, no. 2, pp. 468–478, 2018, doi: 10.1016/j.ijrobp.2018.01.114.

[33] P. Trajdos and M. Kurzynski, "Weighting scheme for a pairwise multi-label classifier based on the fuzzy confusion matrix," *Pattern Recognition Letters*, vol. 103, pp. 60–67, 2018, doi: 10.1016/j.patrec.2018.01.012.

[34] R. S. Samosir, E. Abdurachman, F. L. Gaol, and B. S. Sabarguna, "Hybrid method architecture design of mri brain tumors image segmentation," *ICIC Express Letters*, vol. 14, no. 12, pp. 1177–1184, 2020, doi: 10.24507/icicel.14.12.1177.